ACS OMEGA

http://pubs.acs.org/journal/acsodf

Article

# Impact of Processing Parameters on Contactless Emulsification *via* Corona Discharge

Amir Dehghanghadikolaei, Bilal Abdul Halim, and Hossein Sojoudi*

Cite This: *ACS Omega* 2023, 8, 24931−24941

Read Online

ACCESS | Metrics & More | Article Recommendations | Supporting Information

**ABSTRACT:** A contactless emulsification method is presented using corona discharge. The corona discharge forms using a pin-to-plate configuration, creating a non-uniform electric field. This results in a simultaneous electrohydrodynamic (EHD) pumping of silicone oil and an electroconvection of water droplets that accelerate and submerge inside the oil, leading to a continuous water-in-oil (W/O) emulsion formation process. The impact of the oil viscosity and corona generating AC and DC electric fields (*i.e.*, voltage and frequency) on the characteristics of the emulsions is studied. The emulsification power consumption using the AC and DC electric fields is calculated and compared to traditional emulsion formation methods. While using the DC electric field results in the formation of uniform emulsions, the AC electric field is readily available and uses less power for the emulsification. This is facile, contactless, and energy-efficient for the continuous formation of W/O emulsions.

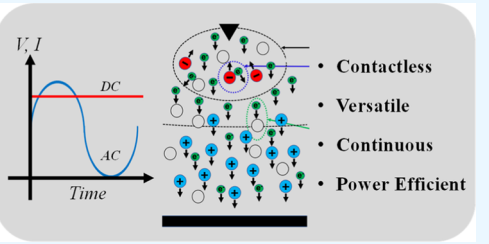


## 1. INTRODUCTION

An emulsion is a colloidal dispersion of one immiscible liquid into another one, forming dispersed and continuous phases, also known as internal and external phases, respectively.[1,2] The emulsions are categorized based on their compositions and droplet sizes of the dispersed phase ($d$). These categories are macro-emulsions, nano-emulsions, and micro-emulsions, with droplet sizes ranging from 0.5 to 100, 0.1 to 1, and 0.01 to 0.1 $\mu$m, respectively. Based on the composition, the emulsions are known to be either oil-in-water (O/W), water-in-oil (W/O), oil-in-water-in-oil (O/W/O), or water-in-oil-in-water (W/O/W).[3−6] Despite what the terms might suggest, the nano-emulsions have droplet sizes that are larger than the micro-emulsions.[7−9] Chemical and physical properties of the continuous and/or dispersed phases (*i.e.*, thermal conductivity, electrical conductivity, polarity, density, viscosity, temperature sensitiveness, *etc.*) impact the properties and stability of the emulsions.[10,11] To form stable emulsions, stabilizer agents such as surfactants are needed to maintain the two immiscible phases next to each other for a longer time.[12] The surfactants or emulsifier compounds can be water- or oil-soluble, depending on continuous and dispersed phases.[13−16]

Based on the required energy, emulsion formation can be categorized as high-energy (HE) and low-energy (LE) processes. Major HE processes are high-pressure homogenization (HPH) and ultrasonic mixing (US), and common LE methods are phase inversions by temperature or chemical composition (PIT and PIC, respectively) and spontaneous emulsification (SE).[17−21] The HE and LE emulsification processes require energy densities of $10^8$ to $10^{10}$ and $10^3$ to $10^5$ W/kg, respectively.[22] Based on the desired emulsion and composition of its phases, as well as operating pressure and temperature, HE or LE emulsification processes are chosen. For example, to obtain large volumes of emulsions with low concentrations of surfactants, high-pressure processes are preferred. However, due to the limitations in the size of the orifices or the ultrasonic probes, several rounds of processing might be required.[23] On the other hand, the LE methods produce more homogeneous emulsions with fine droplets, but they are sensitive to the processing temperatures and to the chemical composition of the continuous and dispersed phases. In addition, the process is sensitive to other properties of the two phases, such as hydrophilic-lipophilic balance (HLB), critical micelle concentration (CMC), *etc.* Which further limits their selection.[24] Furthermore, the LE processes require a higher concentration of surfactants which might lead to unsafe products for applications such as cosmetics.[25,26] Not neglecting their promising performances, the introduced emulsification processes have their own limitations, such as sensitivity to processing conditions, large size of droplets, and alteration of product properties under extreme pressure or high concentrations of unwanted chemical compounds.[27] In addition, neither of the HE or LE methods is capable of forming emulsions continuously.[28]

A reliable alternative to flow-induced droplet breakup or chemical alteration of the phases could be an electro-

Received: February 28, 2023
Accepted: June 7, 2023
Published: July 6, 2023





https://doi.org/10.1021/acsomega.3c01369
*ACS Omega* 2023, 8, 24931−24941

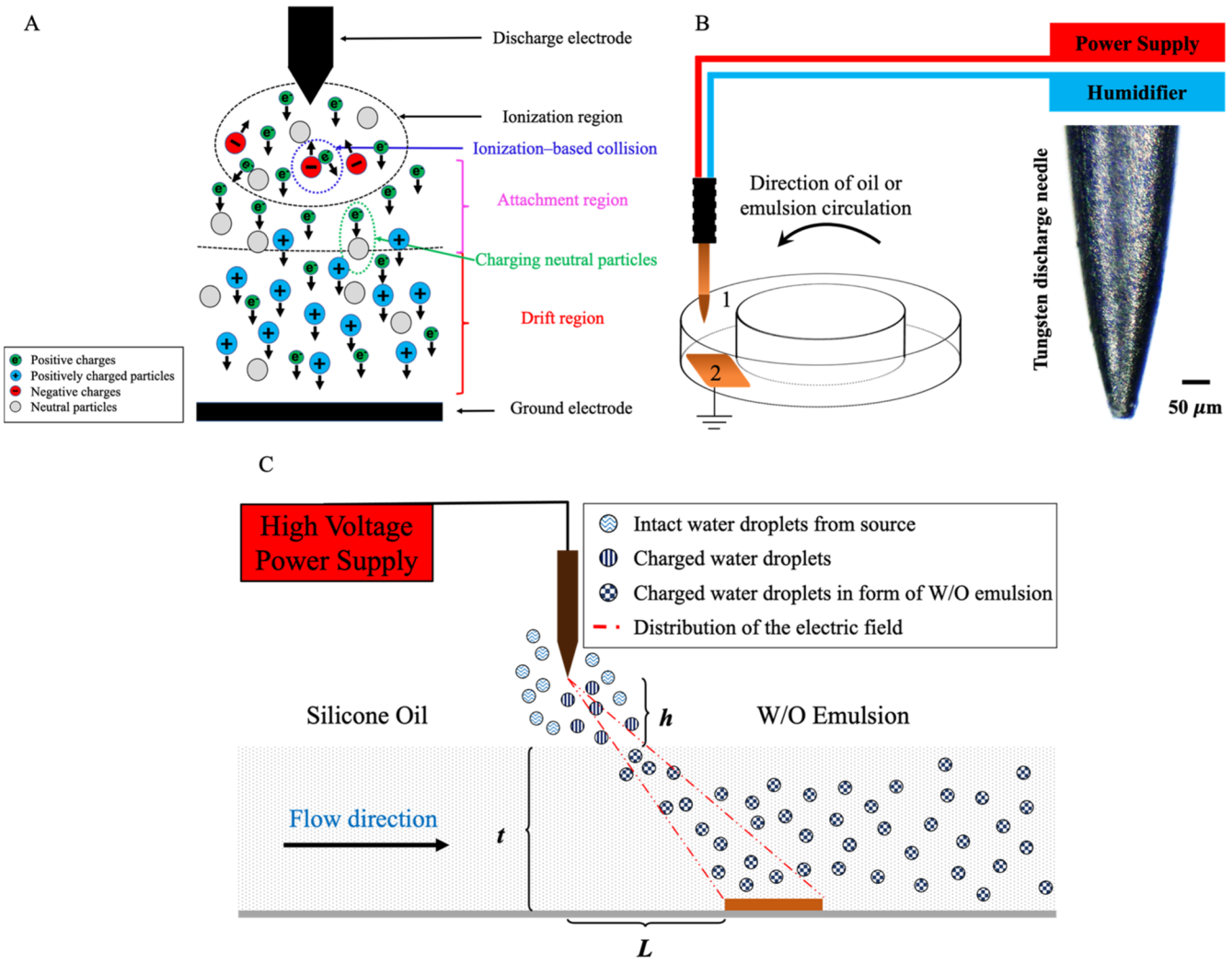


**Figure 1.** (A) Schematic of the ionization process in a pin-to-plate configuration in the corona discharge region showing the formation and release of the charges, ionization, charge collision, and drift of the charged particles toward the ground electrode. (B) Schematic showing components of the corona-assisted electroemulsification setup. (C) Schematic of the corona-assisted emulsification process. The tiny water droplets produced by a humidifier are introduced to the ionization region of the corona discharge. The charged droplets accelerate toward the oil medium, diffusing inside through an electroconvection process. This, combined with EHD pumping of the silicone oil, leads to continuous emulsification. ($h$) and ($L$) are respectively the vertical and horizontal distances between the two electrodes, and ($t$) is the depth of the oil. (1) sharp corona discharge needle and (2) flat ground electrode submerged under the oil phase. Adapted in part with permission from ref 35. Copyright 2022 ACS Omega.

emulsification processes, which is considered more efficient and economical while working with higher viscosity and lower electrical conductivity of the continuous phases.[29] In electro-emulsification, liquid manipulation and droplet breakup are done by an external electric field with no mechanical shearing or change of chemical composition or temperature. Although some safety constraints must be applied to the electro-emulsification processes, the overall flexibility of these processes is superior when compared to the conventional HE and LE methods.[30] This flexibility also enables the formation of designed W/O/W or O/W/O emulsions with desired chemical compositions and controlled droplet sizes over a wide range of viscosities.[31] In addition, electroemulsification processes are considered significantly more energy efficient when compared to the HE methods.[32] Regardless of the flexibility and energy efficiency, it has been reported that more stable emulsions are produced due to the residual built-up charges in the dispersed droplets.[33] However, electroemulsification processes suffer from a critical disadvantage in which certain sets of processing parameters might lead to the coalescence of the emulsion droplets opposite to the intended emulsion formation. While careful adjustment of the experimental parameters and modifications to the setup design, such as using a rotary drum or a magnetic stirrer, can mitigate the electrocoalescence, it cannot be fully prevented.[34]

To address the shortcomings of conventional electro-emulsification processes, we recently reported a novel method of contactless and continuous emulsion formation using corona discharge.[35,36] Corona discharge is a type of cold plasma with a spectrum of blue color, depending on the discharge voltage that results from a discharge under a high potential gradient.[37] Different configurations of corona discharge have been presented in the literature, from which the pin-to-plate configuration is taken in our work.[38] When a sharp conductive needle is connected to a high voltage source and is facing a flat ground electrode, the high potential gradient ionizes the media around the needle that is accelerating toward the ground electrode, forming the corona discharge. The


https://doi.org/10.1021/acsomega.3c01369
ACS Omega 2023, 8, 24931−24941

ionized media could be dry air, air, humidity in form of tiny water droplets, or inert gases.[39] Since the ionized particles/molecules have mass when they travel toward the counter/ground electrode, they produce a flow in the ionized medium, which is known as an ionic wind.[40] During this process, a non-uniform electric field forms, resulting in a negative corona discharge. By placing the ground electrode inside a dielectric liquid and applying the voltage, the liquid can be pumped. This process is known as electrohydrodynamic (EHD) pumping.[41] Here, the corona discharge is utilized for EHD pumping of silicone oils *via* circular motions. The corona discharge also accelerates tiny water droplets (produced by a humidifier) toward the circulating silicone oil. The combination of these two phenomena results in the injection of water droplets into a mixture of silicone oil (with added surfactants), leading to a continuous and contactless emulsification process.

Here, the impact of processing parameters such as the viscosity of silicone oil on emulsion properties are investigated under direct current (DC) and alternating current (AC) electric fields. The frequency of the AC electric field and its impact on the droplet sizes of the dispersed phase are also investigated. The power consumption of corona emulsification under DC and AC electric fields is also studied. While using the DC electric field results in more uniform emulsions with fine droplets, the AC electric field leads to emulsion formation with less power consumption. In addition, the general availability of AC electric fields is another advantage of using this method for electro-emulsification. This study paves the path for a continuous, contactless, reliable, and energy-efficient emulsification process with potential applications in food preservation products,[42] cosmetics and skin care,[43,44] and smart drug delivery.[45,46] Furthermore, the formed emulsions can be practical for a wide range of other applications in the food packaging industries,[47] on demand catalysis of processes,[48] and formation of nano- or micro-reinforced structures[49] and engineered materials for surface treatment applications.[50]

## 2. RESULTS AND DISCUSSION

The external electric non-uniform field formed upon corona discharge causes the carrier medium to move forward as the charged objects hit its surface. In this case, the silicone oil used as the continuous phase has a considerably high electrical resistance ($1 \times 10^{-16}$ S/m), which makes it suitable for the purpose of EHD pumping.[51] Upon charged object-oil impacts, the surface of the silicone oil deforms to different extents, varying from a slight deformation on the top surface to the formation of deep cones reaching to the submerged ground electrode. A DC corona voltage of 10 kV and a sine wave AC corona voltage of 0−+10 kV with varying frequencies of $f$ = 1, 10, 100, 1000, and 10,000 Hz are utilized while studying the impact of the kinematic viscosity of silicone oil ($\nu$ = 50, 100, 200, 350, and 1000 cSt) on the characteristics of the formed emulsion. The used setup is shown in Figure 1. Upon applying the corona voltage, water droplets (formed by the humidifier) obtain charges in the ionization region and accelerate toward the silicone oil medium, diffusing inside. This process is called electroconvection of the water droplets. On the other hand, the corona voltage leads to EHD pumping of the silicone oil while preventing/minimizing its deformation (Taylor cone formation[45]). These two processes occur concurrently, leading to continuous W/O emulsion formation that is collected downstream of the circular setup (Figure 1C). Depending on the processing parameters, the size of the water droplets ($d$) and their uniformity in the formed emulsion change. The different processing conditions are presented in Table 1.

**Table 1. Corona-Assisted Electroemulsification Process Parameters**[a]

| parameter | symbol | range | combination of other parameters |
|---|---|---|---|
| voltage (DC) | $V_{DC}$ | 10 kV (DC) | $h$ = 15 mm, $L$ = 20 mm, $t$ = 8 mm |
| voltage (AC) | $V_{AC}$ | 0−10 kV (AC) | $h$ = 15 mm, $L$ = 20 mm, $t$ = 8 mm, $f$ = 100 Hz |
| kinematic oil viscosity | $\nu$ | 50−1000 (cSt) | $h$ = 15 mm, $L$ = 20 mm, $t$ = 8 mm, $f$ = 100 Hz/DC |
| frequency | $f$ | 1−10,000 (Hz) | $h$ = 15 mm, $L$ = 20 mm, $t$ = 8 mm, $\nu$ = 50 cSt |

[a] $L$ and $h$ are the horizontal and vertical distances between the electrodes (needle tip and ground electrode), $t$ is the depth of the silicone oil, and $f$ is the frequency of the AC electric fields, and $\nu$ is the kinematic oil viscosity.

**2.1. Effect of Oil Kinematic Viscosity ($\nu$) on Water Droplet Size ($d$) under DC Corona Voltage.** The corona discharge is a non-thermal type of plasma discharge that has no effect on the viscosity of the silicone oils. Under given corona operating parameters, an increase in oil viscosity leads to a decrease in the circulation velocity of the oil. In a separate study, we showed that *Reynolds* number *vs* corona voltage follows a power-law trend.[52] In this study, it was found that in order to achieve different EHD-induced motions in the oil medium, different voltages as well as different oil viscosities should be utilized.[53] Lower oil viscosities facilitate penetration and diffusion of the charged water droplets since they have nearly the same value for surface tension while showing less viscous resistance.[54−56] Figure 2A shows the size of the water droplets in W/O emulsions formed under DC corona discharge of $V$ = +10 kV and processing conditions of $h$ = 15 mm, $L$ = 20 mm, and $t$ = 8 mm for silicone oils with different viscosities. A representative optical microscopy image of an emulsion made with $\nu$ = 50 cSt silicone oil along with its high-resolution image are shown in Figure 2B. In addition, a real photo of an emulsion made under these conditions and stored in a glass vial is presented within the plot.

As it can be seen from Figure 2A, with an increase in the oil viscosity from 50 to 1000 cSt, the average water droplet sizes increase from nearly 20−100 $\mu$m. In addition, with an increase in oil viscosity, the variations in water droplet sizes become wider, leading to less uniform emulsions. During the corona-assisted emulsification, the charged water droplets that enter the oil medium are carried away by the EHD pumping of the silicone oil through a circular motion. When the oil viscosity is lower, its circulation velocity is higher. This means that the water droplets entering the high-speed oil do not have any chance to coalesce with the newly entered droplets while being carried away during the emulsification process. In addition, it is hypothesized that inside a less viscous oil, the water droplets with the same sign of charge experience less resistance/drag enabling them to move freely and repel each other easily. Overall, these two effects lead to smaller sized water droplets that are more uniform (comparable to the sizes of feed water droplets) when forming emulsions with less viscous oil.

In some cases, it is possible for the water droplets to become trapped close to the ground electrode and, instead of a circular movement, experience a bounce up and down motion while


https://doi.org/10.1021/acsomega.3c01369
ACS Omega 2023, 8, 24931−24941

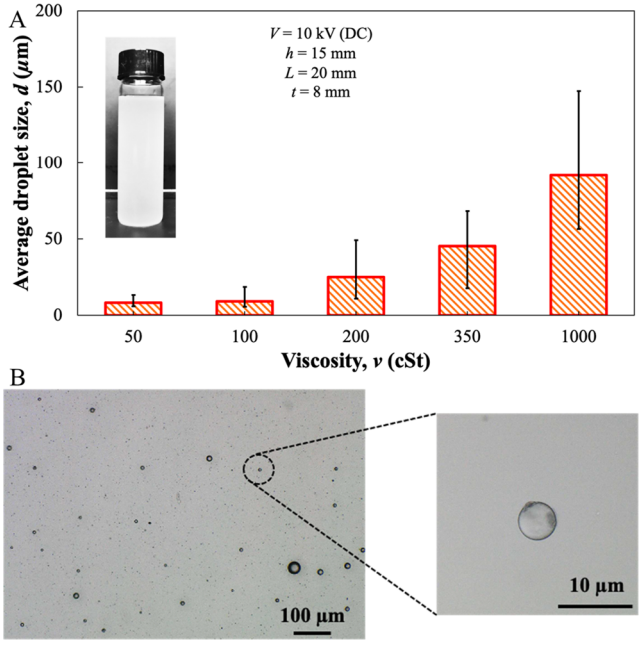


**Figure 2.** Impact of oil viscosity ($\nu$) on the size distribution of water droplets ($d$) inside the emulsion under a DC electric field. The experiments were conducted on silicone oils with kinematic viscosities of $\nu$ = 50, 100, 200, 350, and 1000 cSt under a constant voltage of $V$ = +10 kV (DC), horizontal and vertical electrode distances of $h$ = 15 mm and $L$ = 20 mm, respectively, and oil depth of $t$ = 8 mm. (A) Plot showing the effect of oil viscosity on the size distribution of the water droplets in the W/O emulsion. Inset is a representative photo of the formed emulsion. Decreasing the oil viscosity leads to the formation of more uniform emulsions with fine water droplets. (B) Shows a representative optical microscopy image of an emulsion formed using a 50 cSt viscous silicone oil, along with its high-resolution image to the right.

becoming charged and discharged by touching the ground electrode or the oil surface.[57,58] In these cases, the newly added water droplets might have opposite charges when compared to the previously injected ones, leading to their coalescence and the formation of larger droplets.[59] This electrocoalescence process can continue to an extent where a large sedimentation of the water phase occurs close to the ground electrode, ultimately transforming the corona discharge into an arc discharge. Here, processing parameters are chosen in a way to avoid any arc discharge formation, but the enlargement of the droplets in the oil medium is inevitable in some cases. For example, when the silicone oil is circulating very slowly due to its high viscosity, coalescence in some water droplets might occur, leading to an overall increase in size and higher non-uniformity.

It is to be noted that an upper limit kinematic viscosity of $\nu$ = 1000 cSt is chosen to ensure its EHD pumping despite very low circulation velocities, although the majority of the fluid motion was observed in the middle of the channel.[60] At such high oil viscosity, many of the water droplets become trapped and consumed by the larger ones; however, some droplets still find a path to escape the discharge zone, forming an emulsion that suffers from both an increased average droplet size and a considerable lack of uniformity. It can be seen that the smallest measured droplets in the emulsions made of 1000 cSt silicone oil are nearly equal to the largest ones made with 350 cSt one (see Figure 2A).

**2.2. Effect of Oil Viscosity ($\nu$) on Water Droplet Size ($d$) under AC Corona Voltages.** Similar to the electro-emulsification under DC corona voltages, the electroconvection and the EHD pumping play a major role in forming W/O emulsions under AC corona voltages as well. Both under DC and AC corona voltages, non-uniform electric fields form within the medium (*i.e.*, silicone oil and/or W/O emulsion), leading to the existence of dielectrophoretic (DEP) forces in addition to electrophoretic (EP) forces and dipole−dipole interaction that all contribute to the movement of the water droplets.[61−63] The DEP forces are mainly in charge of droplet elongation, and the EP forces govern separating (and occasionally coalescencing) the charged-neutral particles/droplets. However, both forces play a role in the elongation and separation of the droplets, but to different extents.[64−66] Other than the electric field intensity, the EP and DEP forces also depend on the size of the water droplets and the distance between them. As the water droplets become smaller or are placed farther away, the exerted EP and DEP forces on them decrease.[67−69] These forces exist during corona emulsification under DC applied voltages, but their impacts are negligible. However, when using AC corona voltages, both the EP and the DEP forces play a major role, particularly at lower frequencies. On the other hand, although the EP and DEP forces elongate the droplets and increase the chances of droplet capillary breakage (decreased droplet size in the emulsions), their effects are negligible in higher viscosity silicone oils due to existence of higher drag forces.[70−72] In general, the EP forces form when the charged particles/droplets get neutral charge/s by touching either of the electrodes/poles of the electric field, causing them to move toward a higher potential and consequently experience severe deformations. As this process continues, the elongation causes necking and pinch-off in the deformed droplets.[73,74] On the other hand, the DEP forces occur due to a significant difference in potential between the two poles (*i.e.*, a large potential gradient), which always attracts the droplets in the direction of the strongest pole of the field.[75,76] In this study, the strongest pole is the discharging needle, and the direction of the droplet elongation is always upward (due to the DEP forces), regardless of the direction of the electric field (in the case of using an AC field). As a result, depending on the conditions in the discharge zone (*i.e.*, oil viscosity, fluid circulation velocity, and number of already diffused water droplets), either of these forces can act to deteriorate the quality of the emulsions with coalescence and enlargement of the water droplets.[77] A detailed schematic of the EP and DEP forces is illustrated in Figure S2.

These differences required studying the effectiveness of AC corona voltages for electroemulsification purposes. To this end, an AC applied voltage with an amplitude of 10 kV frequency ranging from 1 to 10,000 Hz was utilized using the sinusoidal function of $V(T) = \frac{V_m}{2}\cos(2\pi fT + \phi) + \frac{V_m}{2}$, where $V_m$ is the amplitude voltage, $f$ is the frequency of the wave, $T$ is the time at which the voltage is being calculated, and $\phi$ is the phase difference of the wave. In the specific case of this study, the phase difference for all the AC experiments was kept constant at $\phi = \pi/2$ With the variations in processing time, the applied AC voltages change from 0 to +10 kV. From AC voltages, a root mean squared voltage ($V_{RMS}$) could be derived which is considered equal to a DC voltage with the same value. For these experiments, the AC voltages were set between 0 and +10 kV, which yields a $V_{RMS}$ of ≈3.5 kV.


https://doi.org/10.1021/acsomega.3c01369
ACS Omega 2023, 8, 24931−24941

Since AC electric fields have many applications in demulsification processes, it is important to consider the alternating current directions in AC electric fields in order to prevent coalescence (a reverse process of emulsification).[78,79] For the experiments using AC corona voltages, the processing conditions were set similar to the previous ones with a working frequency of $f$ = 100 Hz. The reason for selecting this specific frequency was that at lower frequencies, it has been observed that the circulation of the oil medium was slow and inefficient. For higher frequency values, the corona needle started making whizzing sounds, and for safety reasons, it was preferred to avoid working with higher frequencies for a long time. However, in the following discussions, the effect of higher and lower frequencies is investigated in detail. Figure 3A shows

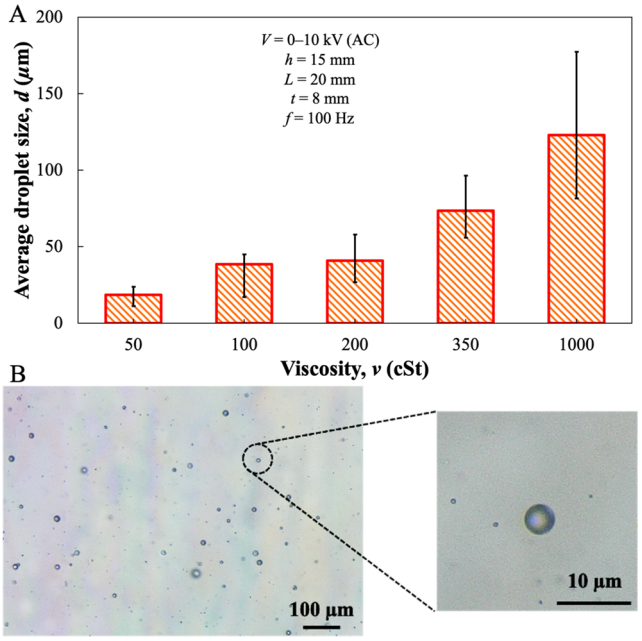


**Figure 3.** Impact of oil kinematic viscosity ($\nu$) on the size distribution of water droplets ($d$) inside the emulsion under an AC electric field. The experiments were conducted on silicone oils with kinematic viscosities of $\nu$ = 50, 100, 200, 350, and 1000 cSt under a sine wave AC voltage of $V$ = 0/+10 kV with a frequency ($f$) of 100 Hz, horizontal and vertical distances of $h$ = 15 mm and $L$ = 20 mm, respectively, and an oil depth of $t$ = 8 mm. The corresponding $V_{RMS} \approx$ 3.5 kV was calculated for these experiments. (A) Effect of oil viscosity on the size distribution of the water droplets in W/O emulsion. Similar to the DC voltage, decreasing the oil viscosity leads to the formation of uniform emulsions with fine sized water droplets. (B) Representative optical microscopy image of an emulsion formed using a 50 cSt viscous silicone oil, along with its high-resolution image at right.

the average droplet sizes and their size distributions under an AC corona voltage of 100 Hz and using silicone oil with varying viscosities. Figure 3B shows a representative optical microscopy image of an emulsion made with 50 cSt viscous silicone oil, along with its high-resolution image at right.

As can be seen from Figure 3A, more uniform emulsions with smaller-sized water droplets were obtained using a 50 cSt silicone oil. With an increase in oil viscosity, corona-assisted electroemulsification resulted in a non-uniform emulsion with significantly increased sizes of the water droplets. This is similar to the trend observed when studying the impact of oil viscosity under DC corona voltages, which can be explained by less drag forces exerted on water droplets in a less viscous oil, leading to facile droplet movement before experiencing any coalescence with the newly entered water droplets. Other than the average droplet size, the variations of the droplet sizes are increased. It is obvious that the higher limit of the droplet sizes represents the larger droplets formed during the process. On the other hand, the tiny water droplets are continuously fed to the oil medium, and it is expected to have the lower limit of the droplet sizes in proximity to the initially introduced water droplets (*i.e.*, ≈1.62 $\mu$m in diameter). However, many of the fresh droplets get stuck on the surface of the silicone oil as a result of water-oil interfacial tension, the smaller size of the droplets, or resisting viscous forces. Consequently, many of the diffused droplets are significantly larger than their original sizes, especially where the oil viscosity is higher.

Comparing the average droplet sizes obtained under DC and AC electric fields (Figures 2A and 3A), it can be seen that more uniform emulsions with fine water droplets are obtained when using a DC corona voltage. With alternating corona voltages, the silicone oil undergoes a pulsating motion, the extent of which depends on the AC frequency. Movie S1 shows a comparison between a smooth oil flow under a DC voltage compared to a pulsating motion of oil under AC voltages. Therefore, the circular movement of the diffused water droplets becomes disturbed when the direction/intensity of applied voltage/electric field reverses. This leads to enhanced coalescence of the diffused water droplets with newly entered ones, leading to more non-uniform emulsions with larger sizes of droplets.[80,81]

**2.3. Effect of AC Electric Field Frequency ($f$) on Water Droplet Size ($d$).** As discussed earlier, in a corona-assisted electroemulsification process, the corona voltage, along with the electrode distances and the depth of the oil, determine the characteristics of the emulsion. In addition, the alternating frequency ($f$) of AC voltages is an important factor due to its impact on the extent of the EP and DEP forces. To explore this further, an AC corona voltage of $V(T) = 5 \times \cos(2\pi \cdot f \cdot T + \pi/2) + 5$ with varying frequencies of $f$ = 1, 10, 50, 100, 1000, and 10,000 is used to form emulsions under the same other operating parameters (i.e., $h$, $L$, and $t$). The silicone oil viscosity was set at 50 cSt, which showed the best EHD pumping performance in previous sections. Figure 4A shows the average water droplet sizes and their variations as a function of the frequency of the AC voltage. Figure 4B is a representative optical microscopy image of an emulsion formed under 1000 Hz AC frequency, along with its high-resolution image at right.

As it can be seen from Figure 4A, with an increase in the AC frequency, the average size of the water droplets and their variations decrease. With an alternating direction of the voltage/electric field, the fluid (silicone oil/emulsion) experiences a sloshing (back-and-forth) motion inside the circular channel.[82] Given this change in the overall motion of the emulsion, the water droplets inside experience varying EP and DEP forces. The diffused water droplets with non-uniform charges/polarity move upward due to the EP and DEP forces. At lower frequencies, this upward movement cannot be reversed quickly since the direction of the electric field reverses slowly. This leads to the presence of water droplets close to the oil surface, which coalesce with the newly entered droplets, resulting in formation of large droplets inside the emulsion.[83] Considering the Coulombic forces ($F_{EP} \propto d^2$) and Clausius–Mossotti function ($F_{DEP} \propto d^3$), it is known that the


https://doi.org/10.1021/acsomega.3c01369
ACS Omega 2023, 8, 24931−24941

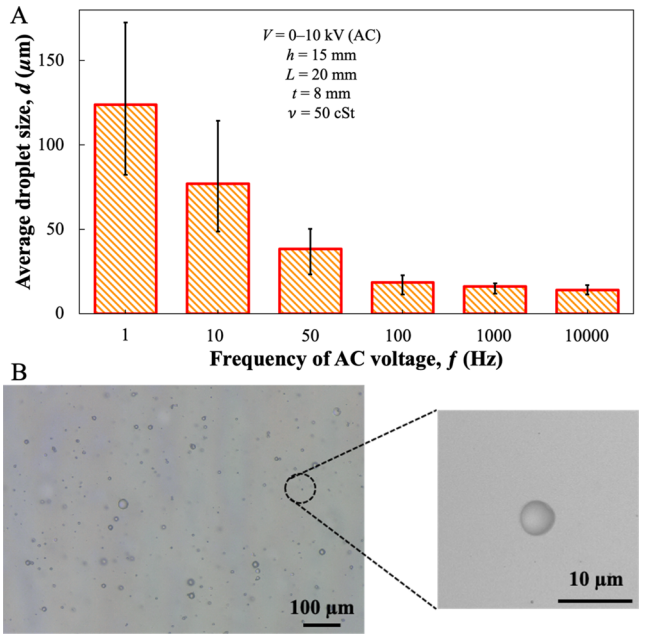


**Figure 4.** (A) Shows how the frequency of AC corona voltage impacts the size distribution of water droplets in the emulsion. The emulsions were formed using 50 cSt silicone oil under AC frequencies of $f$ = 1, 10, 50, 100, 1000, and 10,000 Hz and a voltage of $V$ = 0/+10 kV (AC). The horizontal and vertical distances of the electrodes were $h$ = 15 mm and $L$ = 20 mm, respectively, and the oil depth was $t$ = 8 mm. The corresponding $V_{RMS} \approx 3.5$ kV was calculated for these experiments. As shown, with increasing frequency, both the average size of the droplets and the droplet size variations decrease. (B) Shows a representative optical microscopy image of an emulsion formed under an AC frequency of $f$ = 1000 Hz, along with its high-resolution image at right.

larger droplets tend to exert larger forces in the opposite direction to the electric field.[84−87] As a result, at lower frequencies, the enlarged droplets (*i.e.*, larger $d$ values) go higher, and the cycle of new droplet consumption continues. This phenomenon takes place up to a point where the large droplets change shape from spheres to sediments. Comparing the presented data in Figures 2 and 4, it can be observed that the results for AC and DC-prepared samples are different.

On the other hand, the electric field induces EHD pumping along with electroconvection, which forms the emulsions and moves them out of the discharge region. Since the intensity of the electric fields does not change during the experiments, the applied forward forces to the droplets stay the same. It is obvious that applying equal forward forces results in slower motion of larger droplets compared to smaller ones. In addition to this, knowing the Stoke's law for drag forces, at higher velocities and smaller diameters of droplets, the resisting drag forces are smaller.[88] Combining the effect of a higher drag resistance with a lower propulsion force results in even further slow motion of the larger droplets. Despite changes in the direction of the electric field/voltage, the EHD pumping of the silicone oil/emulsion still occurs. However, a rapidly changing direction in high AC frequencies (*i.e.*, $f \geq 100$ Hz) leads to a visually smooth flow, whereas at low AC frequencies, a sloshing/pulsating flow is observed (see Movie S1).[89] Overall, at AC frequencies lower than $f$ = 100 Hz, the emulsions are non-uniform, with large water droplets.

At higher AC frequencies, the average size of the droplets inside the emulsion is smaller. At these frequencies, the direction of the electric field changes so fast that it does not allow the charged water droplets to bounce up and down due to EP and DEP forces. Instead, the droplets are carried away along with the silicone oil due to the EHD pumping. Fagan *et al.*[90] also have shown that the bouncing behavior of the charged particles under AC electric fields in different electrolytes reaches a relaxation plateau after passing a certain frequency. At such high frequencies, the time for the AC field to repeat is so small that it might resemble a DC electric field, similar to which no sloshing/pulsating behavior is observed in the flow.[73,91] Movie S2 shows the behavior difference of two trapped water droplets at different locations in silicone oil $\nu$ = 50 cSt, and the consequent events.

**2.4. Effect of Processing Parameters on Power Consumption.** The presented corona-induced emulsification is a novel contactless method. However, it is still important to investigate its power consumption rate to compare it with other commercially available processes. Therefore, a series of power consumption measurements were conducted when forming emulsions using a given set of operating parameters. For the cases of DC electric fields, the power consumption values were calculated using Ohm's law; $V = I \times R$ and $P = I \times V$, where $V$ is the applied corona voltage, $I$ is the measured current passing during the discharge, $R$ is the electric resistance, and $P$ is the power consumption value.[92] Since the input voltage is known, only by measuring the current in each experiment can the power consumption be calculated. The results of these measurements are presented in Figure 5A for emulsions formed using DC voltages of $V$ = 3−10 kV and constant parameters of $h$ = 15 mm, $L$ = 20 mm, and $t$ = 8 mm. As expected, the power consumption increases with an increase in the applied voltage. It has been previously shown that at low corona voltages, the EHD pumping is not efficient, and this leads to a non-uniform emulsion formation with large water droplets.[35,36] Since the overall electric resistance between the electrodes stays nearly the same, with increased corona voltage, the current increases and the power consumption increases in a semi-squared ratio compared to the working voltage. Despite an increase in power consumption with an increase in corona voltage, emulsification *via* corona discharge is still very efficient, with power consumptions lower than 1000 mW when compared to other traditional methods of ultrasound-based emulsion formation[93,94] and homogenization.[95]

The measured average power consumption values for the AC experiments are presented in Figure 5B. Similar to the DC experiments, the power was measured using $P = I \times V$, but the RMS values of the current and voltage were used ($P_{average} = I_{RMS} \times V_{RMS}$).[96] At lower frequencies (up to 100 Hz), the power consumption is negligible and reaches a maximum of 338 mW, but at $f$ = 1 kHz, a notable jump occurs and increases the consumed power to nearly 2700 mW. Furthermore, after reaching the highest frequency of 10 kHz, the power consumption completely passes the mW scale and peaks at 16 W. Although the higher frequency values result in higher emulsion uniformity and smaller droplet sizes, the power consumption is extremely high. Referring to the results presented in Figure 4A, it is clearly shown that the average droplet sizes did not change significantly as the operating frequency passed $f$ = 100 Hz. However, if an emulsion with fine droplets is desired, higher power consumption at higher frequencies is involved.

Finally, a simple comparison between the samples made under DC and AC electric fields shows that the power


https://doi.org/10.1021/acsomega.3c01369
ACS Omega 2023, 8, 24931−24941

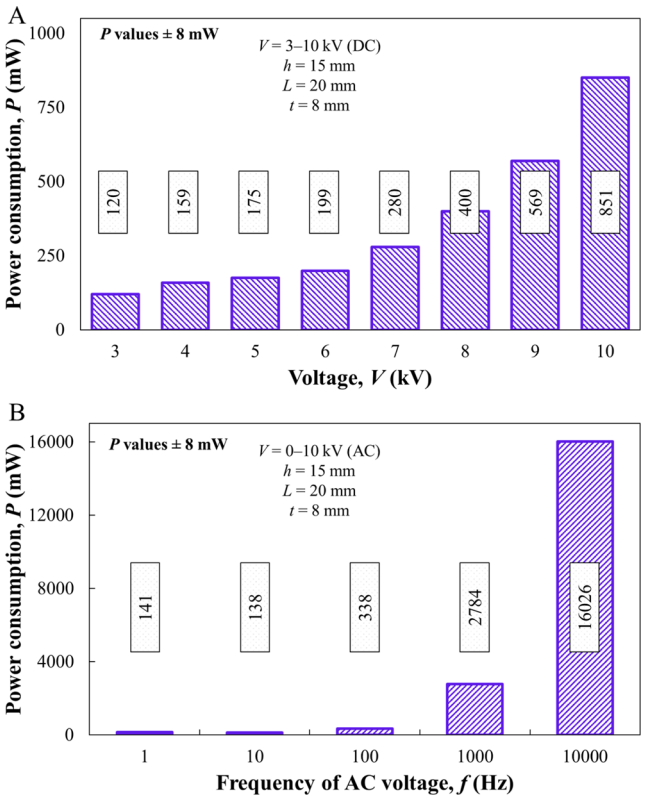


**Figure 5.** Calculated electric power consumption of corona discharge only for samples made under variable voltages and constant processing parameters of $h$ = 15 mm, $L$ = 20 mm, $t$ = 8 mm, and on silicone oil of $\nu$ = 50 cSt viscosity. (A) Calculated power consumption for emulsions made under DC electric fields for variable voltages of $V$ = 3−10 kV and (B) calculated power consumption for emulsions made under AC electric fields with a voltage of $V$ = 0/+10 kV and variable frequencies of $f$ = 1−10,000 Hz.

consumption for samples made under DC electric fields is significantly lower than the ones made under AC electric fields (by keeping all the other processing parameters the same). However, AC currents are available more widely and require less special equipment. On the other hand, if an AC source is used at frequencies around $f \approx 100$ Hz, a high-quality emulsion could be obtained without significantly higher power consumption. The selection of the AC or DC sources is directly tied to the required emulsion quality and power equipment availability. The power efficiency of corona-assisted emulsification is also compared with other commercially available methods. To this end, the calculated power values were divided by the volume of formed emulsions (9 mL) to obtain a volumetric power consumption rate ($\varepsilon$) in W/mL.

As shown in Figure 6, the volumetric power consumption for emulsification using ultrasonic or homogenizer devices is between 2 and 6 W/mL, significantly higher than the values obtained using the corona-assisted emulsification methods.[97,98] For the emulsions made using a 10 kV DC corona voltage, a maximum volumetric power consumption of $\varepsilon$ = 0.295 W/mL was obtained, while that was $\varepsilon$ = 0.261W/mL when using 0/+10 kV AC voltage with a frequency of $f$ = 100 Hz. It is worth noting that the presented values include preprocessing power consumption. The presented results in Figure 6 indicate a considerable power efficiency *via* corona discharge when compared with the reported ultrasonic devices. It is to be noted that some of the low energy emulsification methods are

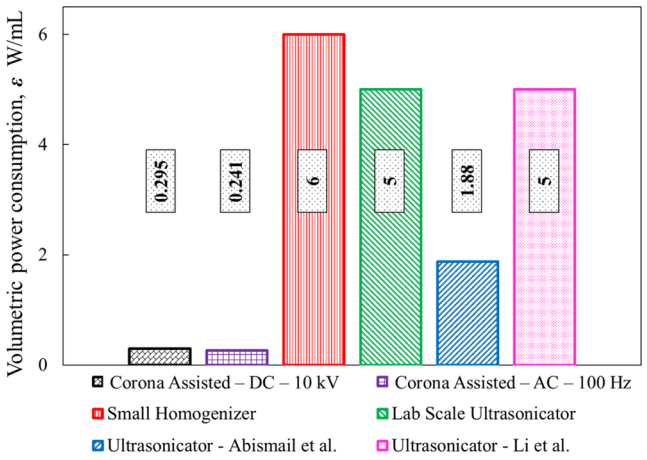


**Figure 6.** Comparison of volumetric power consumption in the corona-induced emulsion formation process and the commonly used ultrasonic and homogenization-based emulsion formation processes. The results of the DC and AC samples, along with the lab-scale homogenizer and ultrasonic device, were measured within the current study, and the rest were provided by the other studies conducted by Li *et al.* and Abismail *et al.* (adapted in part with permission from refs 97 and 98. Copyright 1999 Elsevier). The calculated power consumption for the corona-induced emulsion formation includes the preprocessing power consumption as well.

not considered in this comparison as they rely on phase transformation that requires chemicals and complex equipment.[95,99,100]

In this discussion, different parameters affecting corona-induced emulsion formation were introduced and discussed in depth. It was observed that under DC and AC electric fields, uniform emulsions with small average droplet sizes can be achieved. The optimum working recipe for the experimental conditions can be as follows: $V_{DC}$ = 10 kV, $h$ = 15 mm, $L$ = 20 mm, $t$ = 8 mm, and $\nu$ = 50 cSt. For AC electric fields, the same conditions and a working frequency of $f$ = 100 Hz provide the best uniformity of samples under $V_{AC}$ = 0−10 kV. However, in general, the samples made under $V_{DC}$ yield superior quality. Although it was out of scope of this work, a series of samples were made under the optimum processing conditions and compared to a similar sample made with a lab-scale homogenizer. It was found that corona-assisted emulsion formation yields significantly higher stability over a period of two weeks (Figure S1).

## 3. CONCLUSIONS

In a series of experiments, the effect of different parameters on the defined characteristics of formed emulsions was investigated. Using AC and DC electric fields, it was found that in all cases, a kinematic oil viscosity of $\nu$ = 50 cSt yields the highest quality of emulsion considering its uniformity and the average size of the water droplets. After verification of emulsion formation under AC electric fields, the effect of frequency was investigated. It was revealed that a working frequency of $f$ = 100 Hz can be considered the optimum point, while at frequencies of up to 10 kHz, the average droplet sizes decrease continuously. In addition, it was found that corona-induced emulsion formation provides a significantly more power-efficient method compared to conventionally used techniques (HE methods) while keeping its contactless feature. Throughout the experiments, the following constant process-


https://doi.org/10.1021/acsomega.3c01369
ACS Omega 2023, 8, 24931−24941

ing conditions were used: a vertical distance of $h$ = 15 mm, a horizontal distance of $L$ = 20 mm, and a depth of oil of $t$ = 8 mm. Finally, the most important findings of the current study can be listed as follows:

- Viscosity of the silicone oil significantly affects the emulsion formation process, with the highest uniformity and lowest average droplet size achieved on samples made from silicone oil with $\nu$ = 50 cSt.
- Samples made under DC electric fields yield higher product uniformity and a smaller average droplet size compared to those made under AC electric fields.
- With an increase in the AC frequency (up to $f$ = 10 kHz), the pulsating motion observed in the circular pump decreased, but the behavior was still not identical to that of DC electric fields.
- Although increasing the frequency of AC electric fields improved the quality of the formed emulsions (both uniformity and average droplet size), a threshold point was reached at a working frequency of $f$ = 100 Hz.
- Both AC and DC electric fields provide a power-efficient emulsion formation process, with a slightly higher power consumption for AC electric fields. However, AC is more readily available with less need for special equipment.
- Compared to the conventionally used methods of emulsion formation (ultrasonic emulsion formation, mechanical shearing, and high-pressure homogenization), the proposed corona-assisted method has superior power efficiency both in nominal and volumetric consumption.
- Combining the uniformity of the emulsions, the average size of the water droplets, and the power consumption to form emulsions, it is suggested that a DC voltage of $V_{DC}$ = 10 kV, a vertical distance of $h$ = 15 mm, a horizontal distance of $L$ = 20 mm, a depth of oil of $t$ = 8 mm, and a kinematic oil viscosity of $\nu$ = 50 cSt be used. A similar combination applies to the samples made under AC electric fields with a voltage range of $V_{AC}$ = 0−10 kV.
- Finally, considering the power consumption of each process, its availability, and the quality of the desired emulsions (uniformity and droplet sizes), either DC or AC voltages could be used.

Future work can focus on the effects of other parameters such as different wave forms in the AC electric field, combined pulsed DC and AC electric fields, and surfactant concentration on the characteristics and stability of the formed emulsions.

## 4. MATERIALS AND METHODS

The emulsions were formed using a continuous phase of silicone oils with kinematic viscosities of $\nu$ = 50, 100, 200, 350, and 1000 cSt ($\mu$ MicroLubrol, Clifton, NJ, USA) gently mixed with 1 wt % Span 80 as the surfactant (Sigma Aaldrich, St. Louis, MO, USA). The Span 80 was chosen here due to its abundance and frequent use in various industries such as food, oil processing, cosmetics, and pharmaceutical applications to form stable W/O emulsions.[101,102] The mixture was then placed in an ultrasonic cleaner bath (Vevor, Los Angeles, CA, USA) for 15 min, and this process was repeated three times with 30 min cooling intervals. The cooling process was intentionally added to prevent any property change, as longer periods of ultrasonic mixing might increase the temperature of the mixture. A high-voltage power supply (Siglent, Solon, OH, USA) capable of yielding 10 V along with an amplifier (Advanced Energy, Lockport, NY, USA) capable of increasing the voltage up to a thousand times was used to provide sufficient potential for forming the corona discharge. Both the power supply and the amplifier could provide AC and DC currents. Different DC electric fields were simply obtained using a function generator (Siglent, Solon, OH). For the AC electric fields, a root mean squared voltage ($V_{RMS}$) was used. To get the $V_{RMS}$ values, a commonly used equation ($V_{RMS}$ = $0.353V_{P-P}$) was utilized, where $V_{P-P}$ (peak to peak) is ... is equal to 10 kV in this study.[96]

The pin-to-plate configuration was made using a tungsten needle (Bovie Medical Corporation, Clearwater, FL, USA) connected to the high-voltage input and a grounded copper tape (SparkFun Electronics, Boulder, CO, USA). This configuration is schematically shown in Figure 1A where it also shows the ionization process within the non-uniform electric field generated by the corona discharge. An optical microscope image shows that the needle tip has a diameter of $d_{needle} \approx 45$ $\mu$m that is small enough to form a high gradient of potential when connected to the high voltage input. Although the needle was made from tungsten, regular polishing of the needle tip using sandpaper was conducted to avoid corrosion-caused loss of sharpness.

The EHD pumping setup for circulation of silicone oil and emulsion formation was made of tempered Petri dishes with a glass cap in the center.[35] Figure 1B represents different components of the corona-assisted electroemulsification setup. Other parameters involved in emulsification process are vertical and horizontal distances between the electrodes ($h$ and $L$ in mm), depth of silicone oil ($t$ in mm), and corona voltage ($V$ in kV). The horizontal and vertical distances were measured precisely with an adjustable graduated stand. Mass of added oil was measured using a digital scale (US Solid, Cleveland, OH, USA). Knowing oil density and surface area of the pumping setup, depth of the oil was calculated for each experiment. To provide the humidity (tiny water droplets), a humidifier was used, which could produce water droplets with a diameter of approximately 1.6 $\mu$m.[35] The droplet size measurement was conducted using an environmental particle measurement sensor SPS 30 (Sensirion, Staefa, Switzerland) with an accuracy of ±0.3 $\mu$m. To guide the tiny water droplets toward the ionization region, a flexible polyurethane hose was connected to the outlet of the humidifier and then connected to a location close to the needle tip.

Using the corona setup, the humidifier, and the circular channel, different W/O emulsion samples were made. Emulsion samples for quantification and optical imaging were collected from each quarter of the circular channel (top and bottom layers), for a total of eight collections to ensure accurate sampling. Then, the collected samples were poured into a vial and left for at least 5 h to stabilize before any characterization. All the emulsions were collected after the oil medium completed one round of circulation to ensure equal processing conditions during all experiments. For any given set of experimental combinations, the velocity of the circulating oil changes, and as a result, some of the samples were collected after a significantly longer time. Due to this characteristic of the process, the time of emulsification was not investigated as an independent parameter. After sample collection, the products were poured on clear quartz slides for optical microscopy (Keyence Corporation of America, Itasca, IL, USA). Using ImageJ and Python scripts, the obtained images


https://doi.org/10.1021/acsomega.3c01369
ACS Omega 2023, 8, 24931−24941

were processed, and the size of the water droplets in the W/O emulsions was measured. To ensure achieving the highest accuracy in droplet size measurement, seven different imaging of each sample was conducted, leading to the reported data that is representative of the average of the measured droplet size distributions.

When a non-conductive medium (*i.e.*, silicone oil) is placed between the corona generating and ground electrodes, a non-uniform electric field forms within the medium that can lead to its pumping and/or deformation depending on various processing parameters (*i.e.*, $h$, $L$, $V$, and $t$).[36,45,53] For electroemulsification purposes *via* corona discharge, it is important to achieve efficient EHD pumping of silicone oil without its deformation, which is typically known as Taylor cone formation.[35,103] The deep deformations in the non-conductive silicone oil mostly occur due to extreme EHD forces that appear under certain processing conditions such as very low distance between the two electrodes ($L$ and $h$), low depth of the silicone oil ($t$), very high corona voltages ($V$), *etc.*[104,105] The effects of these processing conditions on the prevention of Taylor cone formation and efficient EHD pumping of silicone oil are presented in our previous studies.[35] Based on these results, a set of processing conditions are chosen to ensure efficient EHD pumping of the silicone oil while studying impact of oil viscosity ($\nu$), nature, and shape of corona operating voltage (DC/AC and its frequency, $f$), and their impact on electroemulsification power consumption. Table 1 summarizes these processing parameters and the range of their values.

## ■ ASSOCIATED CONTENT

### Supporting Information

The Supporting Information is available free of charge at https://pubs.acs.org/doi/10.1021/acsomega.3c01369.

Comparison between a smooth oil flow under a DC voltage and a pulsating motion of oil under AC voltages (MP4)

Behavior difference of two trapped water droplets at different locations in silicone oil $\nu$ = 50 cSt (MP4)

Discussion about the emulsion formation with corona discharge and the affecting phenomena on the dynamics of fluids in the system; set of preliminary results for the stability of the emulsions made with corona discharge and with conventional methods; effect of EHD-induced motion on the properties of formed emulsions; and the active EP and DEP forces and their effects on the scheme of emulsion formation (PDF)

## ■ AUTHOR INFORMATION


### Corresponding Author

**Hossein Sojoudi** − *Department of Mechanical, Industrial, and Manufacturing Engineering, The University of Toledo, Toledo, Ohio 43606, United States;* orcid.org/0000-0002-5278-9088; Email: Hossein.Sojoudi@utoledo.edu

### Authors

**Amir Dehghanghadikolaei** − *Department of Mechanical, Industrial, and Manufacturing Engineering, The University of Toledo, Toledo, Ohio 43606, United States*

**Bilal Abdul Halim** − *Department of Mechanical, Industrial, and Manufacturing Engineering, The University of Toledo, Toledo, Ohio 43606, United States*

Complete contact information is available at: https://pubs.acs.org/10.1021/acsomega.3c01369


### Notes

The authors declare no competing financial interest.

## ■ ACKNOWLEDGMENTS

The authors cordially thank the University of Toledo machine shop and John Jaegly for their help in preparing the setup for safely conducting high-voltage experiments.

## ■ REFERENCES


(1) Yaqoob Khan, A.; Talegaonkar, S.; Iqbal, Z.; Jalees Ahmed, F.; Krishan Khar, R. Multiple emulsions: an overview. *Curr. Drug Deliv.* **2006**, *3*, 429−443.

(2) Akbari, S.; Nour, A. H. Emulsion types, stability mechanisms and rheology: A review. *Int. J. Innovat. Res. Sci. Stud.* **2018**, *1*, 11.

(3) Hou, W.; Xu, J. Surfactant-free microemulsions. *Curr. Opin. Colloid Interface Sci.* **2016**, *25*, 67−74.

(4) Anton, N.; Vandamme, T. F. Nano-emulsions and micro-emulsions: clarifications of the critical differences. *Pharmaceut. Res.* **2011**, *28*, 978−985.

(5) Hejazifar, M.; Lanaridi, O.; Bica-Schröder, K. Ionic liquid based microemulsions: A review. *J. Mol. Liq.* **2020**, *303*, 112264.

(6) do Vale Morais, A.R.; do Nascimento Alencar, É.; Júnior, F.H.X.; De Oliveira, C. M.; Marcelino, H. R.; Barratt, G.; Fessi, H.; Do Egito, E. S. T.; Elaissari, A. Freeze-drying of emulsified systems: A review. *Int. J. Pharm.* **2016**, *503*, 102−114.

(7) Solans, C.; Izquierdo, P.; Nolla, J.; Azemar, N.; Garcia-Celma, M. J. Nano-emulsions. *Curr. Opin. Colloid Interface Sci.* **2005**, *10*, 102−110.

(8) Jiménez Saelices, C.; Capron, I. Design of Pickering micro-and nanoemulsions based on the structural characteristics of nano-celluloses. *Biomacromolecules* **2018**, *19*, 460−469.

(9) Gradzielski, M.; Duvail, M.; de Molina, P. M.; Simon, M.; Talmon, Y.; Zemb, T. Using microemulsions: formulation based on knowledge of their mesostructure. *Chem. Rev.* **2021**, *121*, 5671−5740.

(10) Vargaftik, N. B. *Handbook of Physical Properties of Liquids and Gases-Pure Substances and Mixtures*; Hemisphere Publishing Corporation, 1975.

(11) Boucher, E.; MURRELL, J. *Properties of Liquids and Solutions*; Wiley, 1982.

(12) Kale, S. N.; Deore, S. L. Emulsion micro emulsion and nano emulsion: a review. *Sys. Rev. Pharm.* **2016**, *8*, 39−47.

(13) Modarres-Gheisari, S. M. M.; Gavagsaz-Ghoachani, R.; Malaki, M.; Safarpour, P.; Zandi, M. Ultrasonic nano-emulsification−A review. *Ultrason. Sonochem.* **2019**, *52*, 88−105.

(14) Salehi, F. Physico-chemical and rheological properties of fruit and vegetable juices as affected by high pressure homogenization: A review. *Int. J. Food Prop.* **2020**, *23*, 1136−1149.

(15) Jhalani, A.; Sharma, D.; Soni, S. L.; Sharma, P. K.; Sharma, S. A comprehensive review on water-emulsified diesel fuel: chemistry, engine performance and exhaust emissions. *Environ. Sci. Pollut. Res.* **2019**, *26*, 4570−4587.

(16) Tadros, T. F. Emulsion formation, stability, and rheology. *Emulsion Formation and Stability*; Wiley, 2013; Vol. *1*, pp 1−75.

(17) Li, Y.; Chen, X.; Xue, S.; Li, M.; Xu, X.; Han, M.; Zhou, G. Effect of the disruption chamber geometry on the physicochemical and structural properties of water-soluble myofibrillar proteins prepared by high pressure homogenization (HPH). *LWT–Food Sci. Technol.* **2019**, *105*, 215−223.

(18) Gali, L.; Bedjou, F.; Velikov, K. P.; Ferrari, G.; Donsì, F. High-pressure homogenization-assisted extraction of bioactive compounds from Ruta chalepensis. *J. Food Meas. Char.* **2020**, *14*, 2800−2809.

(19) Taha, A.; Ahmed, E.; Ismaiel, A.; Ashokkumar, M.; Xu, X.; Pan, S.; Hu, H. Ultrasonic emulsification: An overview on the preparation of different emulsifiers-stabilized emulsions. *Trends Food Sci. Technol.* **2020**, *105*, 363−377.

(20) Solans, C.; Morales, D.; Homs, M. Spontaneous emulsification. *Curr. Opin. Colloid Interface Sci.* **2016**, *22*, 88−93.
(21) Preziosi, V.; Perazzo, A.; Caserta, S.; Tomaiuolo, G.; Guido, S. Phase inversion emulsification. *Chem. Eng.* **2013**, *32*, 1585.
(22) McClements, D. J.; Jafari, S. M. Improving emulsion formation, stability and performance using mixed emulsifiers: A review. *Adv. Colloid Interface Sci.* **2018**, *251*, 55−79.
(23) Patrignani, F.; Lanciotti, R. Applications of high and ultra high pressure homogenization for food safety. *Front. Microbiol.* **2016**, *7*, 1132.
(24) Maffi, J. M.; Meira, G. R.; Estenoz, D. A. Mechanisms and conditions that affect phase inversion processes: A review. *Can. J. Chem. Eng.* **2020**, *99*, 178−208.
(25) Jasmina, H.; Džana, O.; Alisa, E.; Edina, V.; Ognjenka, R. *CMBEBIH 2017*; Springer, 2017; pp 317−322.
(26) Yang, Y.; Marshall-Breton, C.; Leser, M. E.; Sher, A. A.; McClements, D. J. Fabrication of ultrafine edible emulsions: Comparison of high-energy and low-energy homogenization methods. *Food Hydrocolloids* **2012**, *29*, 398−406.
(27) Jaworek, A. Electrostatic micro-and nanoencapsulation and electroemulsification: a brief review. *J. Microencapsul.* **2008**, *25*, 443−468.
(28) Karyappa, R. B.; Naik, A. V.; Thaokar, R. M. Electro-emulsification in a uniform electric field. *Langmuir* **2016**, *32*, 46−54.
(29) Ou, G.; Li, J.; Jin, Y.; Chen, M.; Ma, Y.; Gao, K. Behavior Evolution of Droplets Suspended in Castor Oil under Alternating Current Electric Field. *Langmuir* **2022**, *38*, 2084−2093.
(30) Rozynek, Z.; Bielas, R.; Józefczak, A. Efficient formation of oil-in-oil Pickering emulsions with narrow size distributions by using electric fields. *Soft Matter* **2018**, *14*, 5140−5149.
(31) Li, N.; Sun, Z.; Liu, W.; Wei, L.; Li, B.; Qi, Z.; Wang, Z. Effect of electric field strength on deformation and breakup behaviors of droplet in oil phase: A molecular dynamics study. *J. Mol. Liq.* **2021**, *333*, 115995.
(32) Mun, S.; Decker, E. A.; McClements, D. J. Influence of droplet characteristics on the formation of oil-in-water emulsions stabilized by surfactant− chitosan layers. *Langmuir* **2005**, *21*, 6228−6234.
(33) Nawab, M.; Mason, S. The preparation of uniform emulsions by electrical dispersion. *J. Colloid Sci.* **1958**, *13*, 179−187.
(34) Hughes, J.; Pavey, I. Electrostatic emulsification. *J. Electrost.* **1981**, *10*, 45−55.
(35) Dehghanghadikolaei, A.; Shahbaznezhad, M.; Abdul Halim, B.; Sojoudi, H. Contactless Method of Emulsion Formation Using Corona Discharge. *ACS Omega* **2022**, *7*, 7045−7056.
(36) Dehghanghadikolaei, A.; Sojoudi, H.; Abdul Halim, B. Utilization of corona discharge for contactless emulsion formation. *Bulletin of the American Physical Society*; APS, 2022.
(37) Adamiak, K.; Atten, P. Simulation of corona discharge in point−plane configuration. *J. Electrost.* **2004**, *61*, 85−98.
(38) Du, C.; Gong, X.; Lin, Y. Decomposition of volatile organic compounds using corona discharge plasma technology. *J. Air Waste Manage. Assoc.* **2019**, *69*, 879−899.
(39) Chang, J.-S.; Lawless, P. A.; Yamamoto, T. Corona discharge processes. *IEEE Trans. Plasma Sci.* **1991**, *19*, 1152−1166.
(40) Sigmond, R.; Goldman, M. Corona discharge physics and applications. *Electrical Breakdown and Discharges in Gases*; NATO Advanced Study Institute (ASI) Series B; Plenum Press, 1983; Vol. *89*, p 1.
(41) Lai, F. EHD gas pumping−A concise review of recent development. *J. Electrost.* **2020**, *106*, 103469.
(42) Gautam, S.; Lapčík, L.; Lapčíková, B.; Gál, R. Emulsion-Based Coatings for Preservation of Meat and Related Products. *Foods* **2023**, *12*, 832.
(43) Hazt, B.; Parchen, G. P.; do Amaral, L. F. M.; Gallina, P. R.; Martin, S.; Gonçalves, O. H.; de Freitas, R. A. Unconventional and conventional Pickering emulsions: perspectives and challenges in skin applications. *Int. J. Pharm.* **2023**, *636*, 122817.
(44) Guzmán, E.; Ortega, F.; Rubio, R. G. Pickering Emulsions: A novel tool for cosmetic formulators. *Cosmetics* **2022**, *9*, 68.
(45) Mohamed, M. H.; Shahbaznezhad, M.; Dehghanghadikolaei, A.; Haque, M.; Sojoudi, H. Deformation of bulk dielectric fluids under corona-initiated charge injection. *Exp. Fluid* **2020**, *61*, 116.
(46) Wilson, R. J.; Li, Y.; Yang, G.; Zhao, C.-X. Nanoemulsions for drug delivery. *Particuology* **2022**, *64*, 85−97.
(47) Tavassoli, M.; Khezerlou, A.; Bangar, S. P.; Bakhshizadeh, M.; Haghi, P. B.; Moghaddam, T. N.; Ehsani, A. Functionality developments of Pickering emulsion in food packaging: Principles, applications, and future perspectives. *Trends Food Sci. Technol.* **2023**, *132*, 171−187.
(48) Ni, L.; Yu, C.; Wei, Q.; Liu, D.; Qiu, J. Pickering emulsion catalysis: Interfacial chemistry, catalyst design, challenges, and perspectives. *Angew. Chem., Int. Ed.* **2022**, *61*, No. e202115885.
(49) Fresco-Cala, B.; Cardenas, S. Advanced polymeric solids containing nano-and micro-particles prepared via emulsion-based polymerization approaches. A review. *Anal. Chim. Acta* **2022**, *1208*, 339669.
(50) Ahmed, R. M.; Anis, B.; Khalil, A. S. Facile surface treatment and decoration of graphene-based 3D polymeric sponges for high performance separation of heavy oil-in-water emulsions. *J. Environ. Chem. Eng.* **2021**, *9*, 105087.
(51) Shahbaznezhad, M.; Dehghanghadikolaei, A.; Sojoudi, H. Contactless Method for Electrocoalescence of Water in Oil. *ACS Omega* **2021**, *6*, 14298−14308.
(52) Abdul Halim, B.; Dehghanghadikolaei, A.; Amili, O.; Sojoudi, H. Understanding electrohydrodynamic (EHD) performance of corona discharge via particle image velocimetry (PIV). *SN Appl. Sci.* **2023**, *5*, 33.
(53) Abdul Halim, B.; Sojoudi, H.; Amili, O.; Dehghanghadikolaei, A. On the Characterization of Electrohydrodynamic Pumping under DC and AC Corona Discharge Settings. *Bulletin of the American Physical Society*; APS, 2022.
(54) Barca, F.; Caporossi, T.; Rizzo, S. Silicone oil: different physical proprieties and clinical applications. *BioMed Res. Int.* **2014**, *2014*, 502143.
(55) Lee, D.; Choi, D.; Park, H.; Lee, H.; Kim, S. J. Electro-convective circulating flows by asymmetric Coulombic force distribution in multiscale porous membrane. *J. Membr. Sci.* **2021**, *636*, 119286.
(56) Boeuf, J.; Lagmich, Y.; Unfer, T.; Callegari, T.; Pitchford, L. Electrohydrodynamic force in dielectric barrier discharge plasma actuators. *J. Phys. D: Appl. Phys.* **2007**, *40*, 652−662.
(57) Mhatre, S.; Deshmukh, S.; Thaokar, R. M. Electrocoalescence of a drop pair. *Phys. Fluids* **2015**, *27*, 092106.
(58) Chabert, M.; Dorfman, K. D.; Viovy, J. L. Droplet fusion by alternating current (AC) field electrocoalescence in microchannels. *Electrophoresis* **2005**, *26*, 3706−3715.
(59) Mhatre, S.; Thaokar, R. Electrocoalescence in non-uniform electric fields: An experimental study. *Chem. Eng. Process* **2015**, *96*, 28−38.
(60) Kirkgöz, M. S.; Ardiçlioğlu, M. Velocity profiles of developing and developed open channel flow. *J. Hydraul. Eng.* **1997**, *123*, 1099−1105.
(61) Diaham, S.; Valdez-Nava, Z.; Le, T.; Lévêque, L.; Laudebat, L.; Lebey, T. Field Grading Composites Tailored by Electrophoresis—Part 2: Permittivity Gradient in Non-Uniform Electric Field. *IEEE Trans. Dielectr. Electr. Insul.* **2021**, *28*, 341−347.
(62) Green, N. G.; Morgan, H. Separation of submicrometre particles using a combination of dielectrophoretic and electro-hydrodynamic forces. *J. Phys. D: Appl. Phys.* **1998**, *31*, L25−L30.
(63) Shahbaznezhad, M.; Dehghanghadikolaei, A.; Sojoudi, H. Contactless Method for Electrocoalescence of Water in Oil. *ACS Omega* **2021**, *6*, 14298−14308.
(64) Hernandez-Navarro, S.; Tierno, P.; Ignés-Mullol, J.; Sagués, F. AC electrophoresis of microdroplets in anisotropic liquids: transport, assembling and reaction. *Soft Matter* **2013**, *9*, 7999−8004.
(65) Sarno, B.; Heineck, D.; Heller, M. J.; Ibsen, S. D. Dielectrophoresis: Developments and applications from 2010 to 2020. *Electrophoresis* **2021**, *42*, 539−564.


https://doi.org/10.1021/acsomega.3c01369
*ACS Omega* 2023, 8, 24931−24941

(66) Rashed, M. Z.; Williams, S. J. Advances and applications of isomotive dielectrophoresis for cell analysis. *Anal. Bioanal. Chem.* **2020**, *412*, 3813−3833.
(67) Van Dorp, S.; Keyser, U. F.; Dekker, N. H.; Dekker, C.; Lemay, S. G. Origin of the electrophoretic force on DNA in solid-state nanopores. *Nat. Phys.* **2009**, *5*, 347−351.
(68) Wu, Y.; Chattaraj, R.; Ren, Y.; Jiang, H.; Lee, D. Label-Free Multitarget Separation of Particles and Cells under Flow Using Acoustic, Electrophoretic, and Hydrodynamic Forces. *Anal. Chem.* **2021**, *93*, 7635−7646.
(69) Li, X.; Duan, J.; Qu, Z.; Wang, J.; Ji, M.; Zhang, B. Continuous Particle Separation Driven by 3D Ag-PDMS Electrodes with Dielectric Electrophoretic Force Coupled with Inertia Force. *Micromachines* **2022**, *13*, 117.
(70) Zhang, H.; Chang, H.; Neuzil, P. DEP-on-a-chip: Dielectrophoresis applied to microfluidic platforms. *Micromachines* **2019**, *10*, 423.
(71) Zou, J.; Lin, F.; Ji, C. Capillary breakup of armored liquid filaments. *Phys. Fluids* **2017**, *29*, 062103.
(72) McIlroy, C.; Harlen, O. G. Modelling capillary break-up of particulate suspensions. *Phys. Fluids* **2014**, *26*, 033101.
(73) Shahbaznezhad, M.; Dehghanghadikolaei, A.; Sojoudi, H. Optimum operating frequency for electrocoalescence induced by pulsed corona discharge. *ACS Omega* **2020**, *5*, 31000−31010.
(74) Yufa, R.; Krylova, S. M.; Bruce, C.; Bagg, E. A.; Schofield, C. J.; Krylov, S. N. Emulsion PCR significantly improves nonequilibrium capillary electrophoresis of equilibrium mixtures-based aptamer selection: allowing for efficient and rapid selection of aptamer to unmodified ABH2 protein. *Anal. Chem.* **2015**, *87*, 1411−1419.
(75) Han, S.-I.; Huang, C.; Kim, H. S.; Han, A. *2019 IEEE 32nd International Conference on Micro Electro Mechanical Systems (MEMS)*; IEEE, 2019; pp 35−38.
(76) Gao, T.; Zhao, K.; Zhang, J.; Zhang, K. DC-Dielectrophoretic Manipulation and Isolation of Microplastic Particle-Treated Microalgae Cells in Asymmetric-Orifice-Based Microfluidic Chip. *Micromachines* **2023**, *14*, 229.
(77) Jiang, T.; Jia, Y.; Sun, H.; Deng, X.; Tang, D.; Ren, Y. Dielectrophoresis response of water-in-oil-in-water double emulsion droplets with singular or dual cores. *Micromachines* **2020**, *11*, 1121.
(78) Hjartnes, T. N.; Mhatre, S.; Gao, B.; Sørland, G. H.; Simon, S.; Sjöblom, J. Demulsification of crude oil emulsions tracked by pulsed field gradient NMR. Part II: Influence of chemical demulsifiers in external AC electric field. *Colloids Surf., A* **2020**, *586*, 124188.
(79) Wu, D.; Xia, F.; Lin, S.; Cai, X.; Zhang, H.; Liu, W.; Li, Y.; Zhang, R.; Zhang, Y.; Zhang, X.; et al. Effects of secondary emulsification of ASP flooding produced fluid during surface processes on its oil/water separation performances. *J. Petrol. Sci. Eng.* **2021**, *202*, 108426.
(80) Tobazeon, R. Electrohydrodynamic instabilities and electroconvection in the transient and AC regime of unipolar injection in insulating liquids: A review. *J. Electrost.* **1984**, *15*, 359−384.
(81) Kim, J.; Davidson, S.; Mani, A. Characterization of chaotic electroconvection near flat inert electrodes under oscillatory voltages. *Micromachines* **2019**, *10*, 161.
(82) Chen, P. C. Alternating current electrophoresis of human red blood cells. *Ann. Biomed. Eng.* **1980**, *8*, 253−269.
(83) Gabay, I.; Ramos, A.; Gat, A.; Bercovici, M. *APS Division of Fluid Dynamics Meeting Abstracts*; APS, 2021; p A29.007.
(84) Raissi, B.; Marzbanrad, E.; Gardeshzadeh, A. Particle size separation by alternating electrophoretic deposition. *J. Eur. Ceram. Soc.* **2009**, *29*, 3289−3291.
(85) Jones, T. B. Basic theory of dielectrophoresis and electrorotation. *IEEE Eng. Med. Biol. Mag.* **2003**, *22*, 33−42.
(86) Waheed, W.; Sharaf, O. Z.; Alazzam, A.; Abu-Nada, E. Dielectrophoresis-field flow fractionation for separation of particles: A critical review. *J. Chromatogr., A* **2021**, *1637*, 461799.
(87) Urdaneta, M.; Smela, E. Multiple frequency dielectrophoresis. *Electrophoresis* **2007**, *28*, 3145−3155.
(88) Pau, P. C. F.; Berg, J.; McMillan, W. Application of Stokes' law to ions in aqueous solution. *J. Phys. Chem.* **1990**, *94*, 2671−2679.
(89) Vaidyanathan, R.; Naghibosadat, M.; Rauf, S.; Korbie, D.; Carrascosa, L. G.; Shiddiky, M. J.; Trau, M. Detecting exosomes specifically: a multiplexed device based on alternating current electrohydrodynamic induced nanoshearing. *Anal. Chem.* **2014**, *86*, 11125−11132.
(90) Fagan, J. A.; Sides, P. J.; Prieve, D. C. Evidence of multiple electrohydrodynamic forces acting on a colloidal particle near an electrode due to an alternating current electric field. *Langmuir* **2005**, *21*, 1784−1794.
(91) Sojoudi, H.; Shahbaznezhad, M.; Dehghanghadikolaei, A. Emulsion Formation Assisted by Corona Discharge and Electrohydrodynamic Pumping. U.S. Patent 0,355,257 A1, 2022.
(92) Onsager, L. Deviations from Ohm's law in weak electrolytes. *J. Chem. Phys.* **1934**, *2*, 599−615.
(93) Taha, A.; Ahmed, E.; Ismaiel, A.; Ashokkumar, M.; Xu, X.; Pan, S.; Hu, H. Ultrasonic emulsification: An overview on the preparation of different emulsifiers-stabilized emulsions. *Trends Food Sci. Technol.* **2020**, *105*, 363−377.
(94) Potdar, S.; Saudagar, P.; Potoroko, I.; Sonawane, S. *AIP Conference Proceedings*; AIP Publishing LLC, 2022; Vol. *2478*, p 060001.
(95) Gall, V.; Runde, M.; Schuchmann, H. P. Extending applications of high-pressure homogenization by using simultaneous emulsification and mixing (SEM)—An overview. *Processes* **2016**, *4*, 46.
(96) Smith, C. *Environmental Physics*; Routledge, 2004.
(97) Abismaïl, B.; Canselier, J. P.; Wilhelm, A. M.; Delmas, H.; Gourdon, C. Emulsification by ultrasound: drop size distribution and stability. *Ultrason. Sonochem.* **1999**, *6*, 75−83.
(98) Li, W.; Leong, T. S.; Ashokkumar, M.; Martin, G. J. A study of the effectiveness and energy efficiency of ultrasonic emulsification. *Phys. Chem. Chem. Phys.* **2018**, *20*, 86−96.
(99) Yap, B. H.; Dumsday, G. J.; Scales, P. J.; Martin, G. J. Energy evaluation of algal cell disruption by high pressure homogenisation. *Bioresour. Technol.* **2015**, *184*, 280−285.
(100) Sevenich, R.; Mathys, A. Continuous versus discontinuous ultra-high-pressure systems for food sterilization with focus on ultra-high-pressure homogenization and high-pressure thermal sterilization: a review. *Compr. Rev. Food Sci. Food Saf.* **2018**, *17*, 646−662.
(101) Gao, J.; Tong, Z.; Bu, X.; Bilal, M.; Hu, Y.; Ni, C.; Xie, G. Effect of water-in-oil and oil-in-water with Span 80 on coal flotation. *Fuel* **2023**, *337*, 127145.
(102) Ushikubo, F.; Cunha, R. Stability mechanisms of liquid water-in-oil emulsions. *Food Hydrocolloids* **2014**, *34*, 145−153.
(103) Suvorov, V. G.; Zubarev, N. M. Formation of the Taylor cone on the surface of liquid metal in the presence of an electric field. *J. Phys. D: Appl. Phys.* **2003**, *37*, 289−297.
(104) Kamra, A.; Deshpande, C.; Gopalakrishnan, V. Effect of relative humidity on the electrical conductivity of marine air. *Q. J. R. Metereol. Soc.* **1997**, *123*, 1295−1305.
(105) Fernández de La Mora, J. The fluid dynamics of Taylor cones. *Annu. Rev. Fluid. Mech.* **2007**, *39*, 217−243.


https://doi.org/10.1021/acsomega.3c01369
*ACS Omega* 2023, 8, 24931−24941